Angle Images for Measuring Heart Motion from Tagged MRI

Nael F. Osman and Jerry L. Prince
Image Analysis and Communications Laboratory
Department of Electrical and Computer Engineering
The Johns Hopkins University
E-mail: nael@jhu.edu or prince@jhu.edu

Abstract

This paper introduces a new image processing technique for rapid analysis and visualization of tagged cardiac magnetic resonance (MR) images. The method is based on the use of isolated spectral peaks in SPAMM-tagged magnetic resonance images. We call the phase of an image corresponding to just one of these peaks an angle image, and show that except for a phase-wrapping artifact, an angle image is linearly related to a component of the three-dimensional motion. Using one or more angle images, we show how to synthesize conventional tag lines, reconstruct displacement fields for small motions, calculate the optical flow between successive temporal images, and calculate two-dimensional strain. We demonstrate the performance of this approach on both real and simulated tagged MR images.

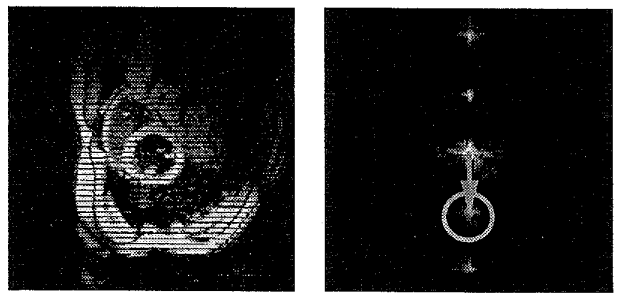

(a) (b)

Figure 1: (a) A 1D SPAMM-tagged image, (b) the magnitude of the Fourier transforms of (a).

1. Introduction

Over the last decade, cardiac imaging using tagged magnetic resonance (MR) imaging has become an established technique in medical imaging [1, 2, 3]. MR tagging (MRT) uses a special pulse sequence to spatially modulate the longitudinal magnetization of the subject prior to acquiring image data. Over many heartbeats acquired in a single breathhold enough data can be acquired to reconstruct an image sequence [4] in which the tag pattern is deformed by the underlying motion of the heart. Usually, the tagging process is thought of as producing saturated planes orthogonal to the image plane, leading to images such as that shown in Fig. 1a. This pattern is called a SPAMM tag pattern [5, 6]; this class of patterns form the basis for the work presented in this paper.

Although significant improvements in the image acquisition methodology have been developed [7, 6, 8, 9, 10], MR tagging is only being slowly adopted in the clinical setting in part because of the lack of fast analytical and visualization techniques. In this paper, we propose a new methodology that is fast, fully-automated, and readily extendable to three dimensions. It is based on the fact that SPAMM-tagged MR images [5, 6] have a collection of distinct spectral peaks in the Fourier domain, and that each spectral peak contains information about the motion in a certain direction. The inverse Fourier transform of just one of these peaks, extracted using a bandpass filter, is a complex image whose phase is linearly related to a directional component of the true motion. We define an *angle image* to be exactly this phase image, except that it is constrained to lie in the range $[-\pi, \pi)$ by the action of the standard inverse tangent operator. Despite this angle-wrapping artifact, an angle image can be used to estimate synthetic tag lines, and pairs of angle images can be used to measure small displacement fields, optical flow in image sequences, and two-dimensional strain. Here, we outline the theory, show some initial experimental results, and describe areas for future research.

This research was supported by the National Institutes of Health (R29-HL47405) and the National Science Foundation (MIP-93-50336).

2. Angle Images

2.1. Complex Images

Fig. 1b shows the magnitude of the Fourier transform of Fig. 1a. The spectral peaks in Fig. 1b arise because the sinusoids in the SPAMM tag pattern amplitude modulate the underlying image, acting as as carriers that shift the underlying spectrum into various positions. The number and distribution of the spectral peaks vary according to the specific tagging pulse sequence, and it can be shown that any SPAMM-tagged image can be written as

$$\psi = \sum_{k=-K}^{K} \psi_k \tag{1}$$

where $2K+1$ is the number of spectral peaks and ψ_k is a complex image that is the inverse Fourier transform of one of the spectral peaks. We now give the specific form of ψ_k and then define the angle image.

First, we require a notation that allows expression of the effects of 3D heart motion on 2D (usually oblique) images. We let $\mathbf{x} \in \mathbb{R}^3$ represent scanner coordinates, a fixed laboratory frame within the magnet. To establish the *orientation* of an image, we define the vectors $\mathbf{h}_1 \in \mathbb{R}^3$ and $\mathbf{h}_2 \in \mathbb{R}^3$ to represent the readout and phase-encoding directions, respectively, of the image plane. By convention we set $\|\mathbf{h}_1\| = \|\mathbf{h}_2\| = 1$ and $\mathbf{h}_1^{\mathrm{T}}\mathbf{h}_2 = 0$. To establish the physical *position* of the image, we let $\mathbf{x}_0 \in \mathbb{R}^3$ be the image origin.

An image point is given by a 2D vector $\mathbf{y} = [y_1\ y_2]^{\mathrm{T}}$, where y_1 gives the image position in the readout direction and y_2 gives the image position in the phase-encode direction. The actual 3D position $\mathbf{x}$ of $\mathbf{y}$ is therefore given by the function

$$\mathbf{x}(\mathbf{y}) = y_1\mathbf{h}_1 + y_2\mathbf{h}_2 + \mathbf{x}_0 = H\mathbf{y} + \mathbf{x}_0 \tag{2}$$

where $H = [\mathbf{h}_1\ \mathbf{h}_2]$. As the heart deforms, the original position $\mathbf{p}$ of a 3D point $\mathbf{x}$ could be found using the *reference map* $\mathbf{p}(\mathbf{x}, t)$, if it were known. The reference map completely characterizes the heart motion and relates all points within an image to their physical positions at the time of tag application.

It is intuitive that local motion would cause the phase of sinusoidal patterns to be locally changed. In fact, the motion produces an angle modulation of the tag pattern, and it can be shown that each complex image has the form

$$\psi_k(\mathbf{y}, t) = D_k(\mathbf{y}, t)e^{j(\mathbf{w}_k^{\mathrm{T}}\mathbf{p}(\mathbf{x}(\mathbf{y}),t)+\theta_k)}\,. \tag{3}$$

Here, D_k is a scalar function representing the underlying image amplitude; $\mathbf{w}_k$ is the location of the spectral peak (see arrow in Fig. 1b); and θ_k is an arbitrary phase determined by the position of application of the tag pattern. Defining the *displacement field* as

$$\mathbf{u}(\mathbf{x}, t) = \mathbf{x} - \mathbf{p}(\mathbf{x}, t) \tag{4}$$

it follows that a complex image can also be written as

$$\psi_k(\mathbf{y}, t) = D_k(\mathbf{y}, t)e^{j(\mathbf{w}_k^{\mathrm{T}}\mathbf{x}(\mathbf{y})+\theta_k)}e^{-j\mathbf{w}_k^{\mathrm{T}}\mathbf{u}(\mathbf{x}(\mathbf{y}),t)}\,. \tag{5}$$

These complex images can be approximately determined by filtering the spectral peaks of tagged MR images using bandpass filters. Alternatively, they can be directly imaged using selective k-space imaging.

2.2. Angle Images

From (3) we see that the phase of ψ_k is

$$\phi_k(\mathbf{y}, t) = \mathbf{w}_k^{\mathrm{T}}\mathbf{p}(\mathbf{x}(\mathbf{y}), t) + \theta_k\,. \tag{6}$$

It it could be determined, the phase image ϕ_k would be extremely useful since it is linearly related to the reference map $\mathbf{p}$, our primary unknown. However, phase-unwrapping would be required to determine ϕ_k from ψ_k, and this is impractical given the high noise level in these images. Instead, we will work with the following images

$$a_k(\mathbf{y}, t) = \angle\psi_k(\mathbf{y}, t)\,, \quad -K \le k \le K \tag{7}$$

which are restricted to the range $[-\pi, \pi)$ and which we call *angle images*. Angle images are easily calculated from the complex images and are related to the true phase images as follows

$$a_k(\mathbf{y}, t) = \mathcal{W}(\phi_k(\mathbf{y}, t))\,, \tag{8}$$

where the nonlinear *wrapping function* is given by

$$\mathcal{W}(\phi) = \mathrm{mod}(\phi + \pi, 2\pi) - \pi\,. \tag{9}$$

Fig. 2a shows two images of the left ventricle taken at end-diastole and shortly after. Fig. 2b shows the corresponding angle images computed from a single spectral peak at each time. The discontinuity in intensity is caused by angle wrapping. It should be noted that both the phase and the angle are material properties of the tagged tissue. In other words, if one follows a particular material point $\mathbf{p}$, its phase and angle remain constant with time.

2.3. Applications

1. Synthetic Tag Lines. The discontinuities in Fig. 2b strongly resemble 1D tag lines. In fact, the lines we see in this figure represent a crude (pixelated) approximation of image isocontours having the value $-\pi$.

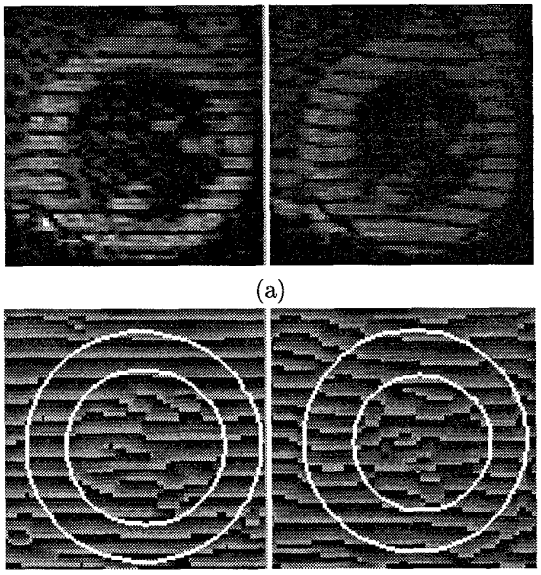

(a)

(b)

Figure 2: (a) Cross section of the left ventricle with planar SPAMM tags, and (b) shows corresponding angle images.

Since the angle of a tagged image is a material property of the tissue, these lines in fact represent samples of surfaces all having the angle $-\pi$. These surfaces are completely analogous to tag surfaces arising from planar tagging or higher-order 1D binomial SPAMM tagging, and the lines are analogous to the intersection of image planes with these tag surfaces. In essence, angle images can be used to generate *synthetic tag lines* by identifying isocontours within the angle images. These lines can then be used in any standard analysis procedure based on planar tags (cf. [6, 11]).

2. Measuring Small Motion. Given complete knowledge of the tagging pulse sequence and given the angle image $a_k(\mathbf{y}, t)$, the following quantity can be calculated

$$\Delta a_k(\mathbf{y}, t) = \angle e^{j(\mathbf{w}_k^{\mathrm{T}}\mathbf{x}(\mathbf{y}) + \theta_k - a_k(\mathbf{y},t))} = \angle e^{j(\mathbf{w}_k^{\mathrm{T}}\mathbf{u}(\mathbf{x}(\mathbf{y}),t))}$$

If $|\mathbf{w}_k^{\mathrm{T}}\mathbf{u}| < \pi$, then no wrapping will occur in the calculation of the angle and

$$\Delta a_k(\mathbf{y}, t) = \mathbf{w}_k^{\mathrm{T}}\mathbf{u}(\mathbf{x}(\mathbf{y}), t) \tag{10}$$

which is the displacement component in the direction $\mathbf{w}_k$. Using another angle image having a linearly independent direction $\mathbf{w}_l$, the displacement field $\mathbf{u}$ is readily determined.

3. Measuring Strain. Strain can be described as the normalized change of fiber length in a direction given by a unit vector $\mathbf{e}$. In the Eulerian sense, this directional strain can be given by

$$\epsilon_2(\mathbf{y}, t; \mathbf{e}) = \|\nabla_{\mathbf{y}}\mathbf{p}(\mathbf{x}(\mathbf{y}), t)\,\mathbf{e}\| - 1 \tag{11}$$

The gradient $\nabla_{\mathbf{y}}\mathbf{p}$ can be computed from the angle images using

$$\nabla_{\mathbf{y}}\mathbf{p} = (W^{\mathrm{T}})^{-1}\begin{bmatrix} \nabla_{\mathbf{y}} a_k^* \\ \nabla_{\mathbf{y}} a_l^* \end{bmatrix}, \tag{12}$$

where the matrix

$$W = [\mathbf{w}_k\ \mathbf{w}_l] \tag{13}$$

and

$$\nabla_{\mathbf{y}} a_k^* = \begin{cases} \nabla_{\mathbf{y}} a_k & \|\nabla_{\mathbf{y}} a_k\| \le \|\nabla_{\mathbf{y}} a_k^{(\pi)}\| \\ \nabla_{\mathbf{y}} a_k^{(\pi)} & \text{otherwise} \end{cases} \tag{14}$$

and

$$a_k^{(\pi)}(\mathbf{y}, t) = \angle e^{j(a(\mathbf{y},t)+\pi)} \tag{15}$$

This last equation is just a trick to avoid the discontinuities in the calculation of the gradient of an angle image.

4. Optical Flow. Optical flow is defined as the apparent motion of brightness patterns in an image sequence [12]. In our case, the word apparent implies motion within the image plane, instead of true 3D motion. It is traditional to define optical flow using velocity fields, and most often some sort of regularization is required in order to get a dense estimate of this velocity field [13]. It is well-known that conventional gradient-based optical flow processing assumes a linear image brightness intensity model and that it generally requires regularization to solve the aperture problem. Angle images provide this approximate linear intensity model (see Fig. 2), and since they can be synthesized in several directions, no regularization is required. Using the brightness constraint equation on angle images from more than one direction, it is possible to set up a matrix equation from which the velocity components can be directly found. A minor problem with wrapped angles is solved by using shifted angle images.

3. Experimental Results

Fig. 3 shows tag lines synthesized using an angle image calculated from one spectral peak of the underlying image. The angle generating the isocontours was deliberately chosen so that its isocontours pass through the valleys of the tag lines. Isocontours outside the LV

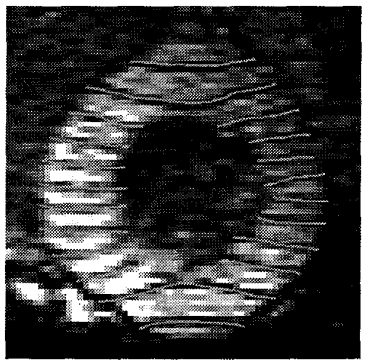

Figure 3: The synthesized tags from a planar tag image

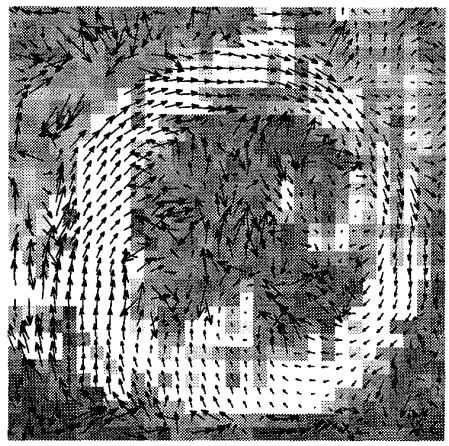

Figure 4: The displacement field from the first to the second frame in systole

wall muscle were removed manually for visualization purposes. Visually, the tags agree well with the tag lines apparent in the image. This shows a single angle image contains quite a bit of information about the motion, although its spectral extent is much smaller than that of the entire tagged image. It should be noted that by taking additional isocontour values, synthetic tag lines lying between the visual tags can be readily generated.

Fig. 4 shows the small displacement field calculated for the right-hand image in Fig. 2a. In this case, a tagged image having vertical tags (not shown) was used to provide the second angle image having a linearly independent direction. Although the computed displacement field actually represents the projection of the 3D displacement on the image plane, since this is a mid ventricular slice, the out of plane component is very small. As shown in the figure, when the tissue of the heart starts contracting, it rotates around the long axis of the heart. Also, there seems to be more rotation at the heart's septum than at the free wall of the LV.

To demonstrate strain computation, we used planar tagged MR images of a paced canine heart, where the pacer was placed at the basal left ventricular free-wall. Two sets of image sequences with horizontal and vertical tags were used. The principle harmonic from each set was used to produce a corresponding angle image. Fig. 5a shows 2D tagged images produced by multiplying the two sets of tagged images for visualization purposes. The circumferential strain was computed at each instant and is shown in Fig. 5b. As shown in the second image of the first row in the strain sequence, early mechanical activation is seen emanating from the pacing site (5 O'clock direction). Notice the significant prestretch (dark color) of the septal region remote from the pacing site.

Due to space limitations, our optical flow result is omitted, but will be shown at the conference.

4. Conclusion

In this paper, we introduced the concept of angle images in cardiac tagged MR imaging. An angle image is the angle-wrapped phase of the inverse Fourier transform of one spectral peak in a SPAMM-tagged MR image. It can be imaged very fast, calculated automatically, and used to compute synthetic tag lines, strain, small displacements, and optical flow. Further angle images can be extended directly to 3D or used in conventional methods to infer 3D motion from 2D images.

Acknowledgments

We thank Mike Guttman, Sandeep Gupta, and Stephanos Androutsellis-Theotokis for their ideas and suggestions; and to Elliot McVeigh, Ergin Atalar, and Anthony Faranesh for providing us with the data used in this paper.

5. References

[1] A. A. Young and L. Axel, "Three-dimensional motion and deformation with spatial modulation of magnetization," *Radiology*, vol. 185, pp. 241–247, 1992.

[2] E. R. McVeigh and E. A. Zerhouni, "Noninvasive measurements of transmural gradients in myocar-

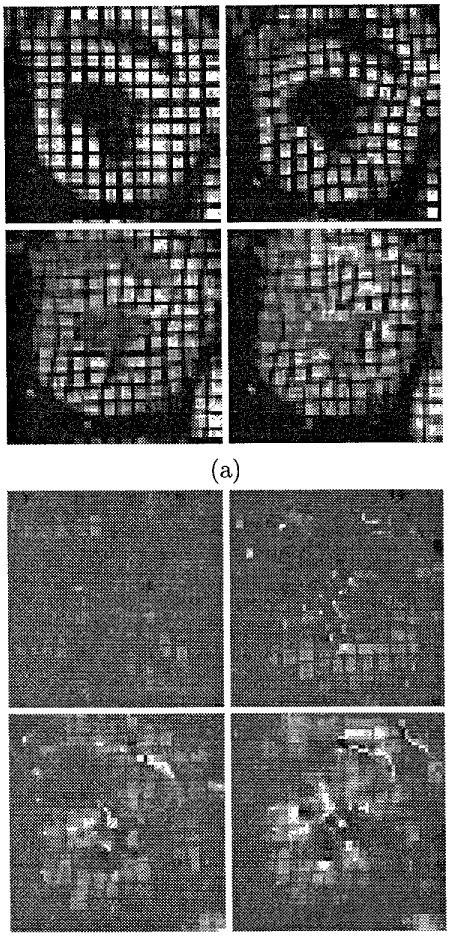

(a)

(b)

Figure 5: (a)The tagged images of a paced canine heart shown from end-diastole at the top left corner to end-systole at the bottom right corner. (b) The corresponding estimated circumferential strain within a cross section of a paced canine heart. Gray regions indicate zero strain; lighter regions indicate contraction; and darker regions indicate stretching.

dial strain with MR imaging," *Radiology*, vol. 180, no. 3, pp. 677–683, 1991.

[3] C. Moore, W. O'Dell, E. McVeigh, and E. Zerhouni, "Calculation of three-dimensional left ventricular strains from biplanar tagged MR images," *Journal of Magnetic Resonance Imaging*, vol. 2, pp. 165–175, Mar/Apr 1992.

[4] E. Atalar and E. R. McVeigh, "Optimization of tag thickness for measuring position with magnetic resonance imaging," *IEEE Trans. Med. Imag.*, vol. 13, no. 1, pp. 152–160, 1994.

[5] L. Axel and L. Dougherty, "MR imaging of motion with spatial modulation of magnetization," *Radiology*, vol. 171, pp. 841–845, 1989.

[6] L. Axel and L. Dougherty, "Heart wall motion: Improved method of spatial modulation of magnetization for MR imaging," *Radiology*, vol. 172, no. 1, pp. 349–350, 1989.

[7] E. McVeigh, "MRI of myocardial function: Motion tracking techniques," *Mag Res Med*, vol. 14, no. 2, pp. 137–150, 1997.

[8] S. E. Fischer, G. c. McKinnon, M. B. Scheidegger, W. Prins, D. Meier, and P. Boesiger, "True myocardial motion tracking," *Magnetic Resonance in Medicine*, vol. 31, pp. 401–413, 1994.

[9] M. Doyle, E. G. Walsh, R. E. Foster, and G. M. Pohost, "Common k-space acquisition: A method to improve myocardial grid-tag contrast," *Mag Res Med*, vol. 37, pp. 754–763, 1997.

[10] S. Zhang, M. Douglas, L. Yaroslavsky, R. Summers,
V. Dilsizen, L. Fananapazir, and S. Bacharach, "A fourier based algorithm for tracking spamm tags in gated magnetic resonance cardiac images," *Medical Physics*, vol. 23, pp. 1359–1369, August 1996.

[11] W. G. O'Dell, C. C. Moore, W. C. Hunter, E. A. Zerhouni, and E. R. McVeigh, "Displacement field-fitting for calculating 3D myocardial deformations from tagged MR images." preprint, 1995.

[12] E. C. Hildreth, *Measurement of Visual Motion.* Cambridge: MIT Press, 1984.

[13] B. K. P. Horn and B. G. Schunck, "Determining optical flow," *Artificial Intelligence*, vol. 17, pp. 185–203, 1981.